

EXPERIMENTAL AND ANALYTICAL STUDIES OF STRENGTHENING USING DRILLED-IN BONDED SHEAR REINFORCEMENT

Mathieu Fiset & Prof. Josée Bastien
Université Laval
Dept. of Civil Engineering
1065 Avenue de la Médecine
Québec, Qc, Canada
Mathieu.fiset.1@ulaval.ca

Prof. Denis Mitchell
McGill University
Dept. of Civil Engineering
817 Sherbrooke Street West
Montréal, QC, Canada

KEYWORDS:

Shear, Bridges, Strengthening, Evaluation, Repair.

ABSTRACT

In order to study means of improving the behaviour of thick slabs without shear reinforcement a series of large-scale beams representing thick slabs was constructed and tested. Companion specimens were strengthened using drilled-in reinforcing bars to study the effectiveness of this repair technique. The behaviour of these beams, before and after strengthening, is compared. An additional experimental program using pull-out specimens enabled a study of the bond characteristics of drilled-in reinforcement having different embedment lengths. An analytical model to predict the bond-stress versus slip relationship enabled the development of a method for predicting the influence of the added shear reinforcement in improving the shear strength. These predictions are compared with the experimental results and provide a practical means of assessing the influence of post-installed shear reinforcement.

INTRODUCTION

On September 30th, 2006, the Concorde overpass (Laval, Qc, Canada) collapsed, killing five people and injuring six others. Even though the original design respected standards at the time, a shear failure in the cantilever region of the supporting concrete thick slab led to the collapse (Johnson et al, 2007). The shear failure mode of unstrengthened thick slabs is very brittle and provides no warning signs of the approaching collapse. For the Concorde overpass collapse, investigations have shown that concrete degradation with time resulted in the propagation of inclined cracking, followed by a shear failure. That event raised questions concerning the safety of many aging concrete thick slab bridges without shear reinforcement. Moreover, the investigation has showed that the minimum amount of shear reinforcement recommended by the current Canadian standard (CAN-CSA, 2006) would have prevented the Concorde overpass collapse (Johnson et al, 2007; Mitchell et al, 2011). Thus, methods to introduce, at least, the minimum amount of shear reinforcement into thick concrete slabs have gain wide interest.

In order to study the behaviour of thick slabs without shear reinforcement, a series of large-scale beams representing thick slabs were constructed and tested (Provencher 2011; Cusson 2012; Fiset et al, 2012). Companion specimens were strengthened using drilled-in reinforcing bonded bars to study the effectiveness of this repair technique. The installation of bonded bars is illustrated in Fig. 1. This involves drilling holes in the concrete element from the top surface, down to the flexural reinforcement (Fig. 1a). The holes need to be cleaned with high pressure air and water (Fig. 1b), and filled with the epoxy adhesive (figure 1c). Thereafter, steel reinforcing bars are inserted into the holes (Fig. 1d). In comparison with other strengthening methods used on narrow beams (De Lorenzis and Nanni, 2001; Adhikary and Mutsoyoshi, 2006; Barros and Dias, 2006; Fernández and al, 2010), the proposed method has the advantage of being effective on wide thick slabs.

Details of the beams that represent portions of thick slabs along with the strengthening details are summarized in Table 1 and Fig. 2. The beams have a 4 m free span, a width, b , of 610 mm and a depth, h , of 750 mm. Slabs B3 and B4 were strengthened with bonded drilled-in shear reinforcement. For comparison purposes, slab S1 contains conventional stirrups installed before concrete casting. Reinforcing bars used for the shear reinforcement were 15M, (diameter of 15.9 mm). Results showed that the shear-strengthened slabs using bonded reinforcement can exhibit failure loads 46% higher compared with companion unstrengthened slabs. However, the predicted shear strength using design provisions of current standards and assuming that the drilled-in reinforcement was fully effective was 29% higher than the experimental results. This observation can be attributed to the diagonal shear crack location. Figure 3 shows the cracking pattern of strengthened slab B2 after failure. The embedded length L_b of the shear reinforcement (dashed line) is determined by the main shear crack location, influencing the maximum tensile stresses developed in the shear reinforcement. It is apparent that some of the bonded reinforcing bars were not fully anchored and therefore unable to develop their full yield strength f_{yv} as assumed by current standards for conventional stirrups.

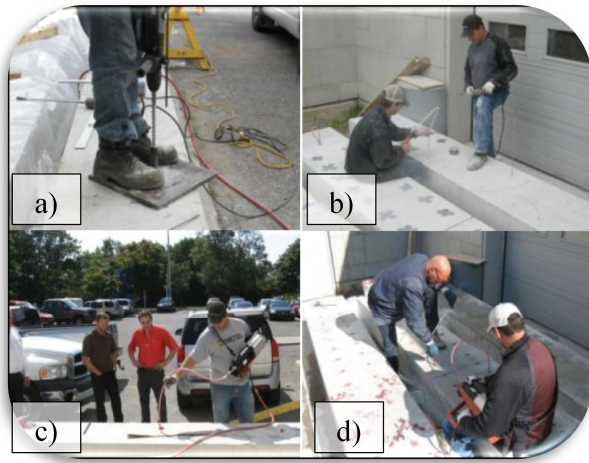


Fig. 1: Installation procedure of bonded shear reinforcement

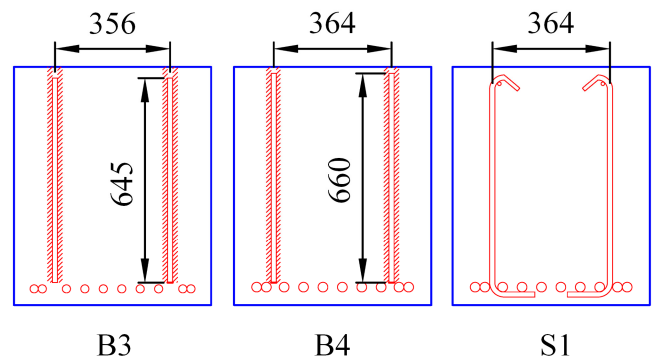


Fig. 2 Cross section of slabs specimens (unit: mm)

Table 1 Details of tested slab specimens

Slabs	Number of tested slabs	h (mm)	d (mm)	ρ_{flex} (%)	s_v (mm)	s_v / d_v	A_v (mm ²)	f_{yv} (MPa)	f_c (MPa)	E_c (MPa)
B3	2	750	698	1.17	470	0.75	400	480	35.6	29395
B4	2	750	694	1.65	380	0.61	400	448	34.5	26315
S1	2	750	694	1.65	380	0.61	400	448	33.3	25704

Objectives

The main objective of the research program is to develop an approach for predicting the increase in shear strength of strengthened thick slabs. First, this paper presents an investigation of the behaviour of epoxy bonded shear reinforcement using pull-out test, associated analytical modelling and finite elements (FE) models. The pull-out tests have been performed to determine the bond-slip behaviour of the bonded reinforcing bars. Secondly, on the basis on this bond-slip behaviour, finite element modelling has been developed with VecTor2 (Wong and Vecchio, 2002) to examine the behaviour of strengthened slabs and its bonded shear reinforcement.

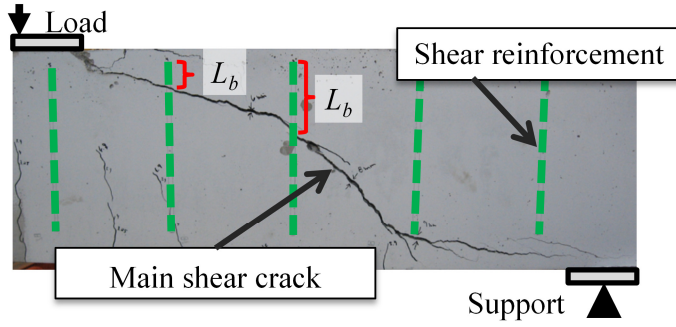


Fig. 3: Failure of slab with bonded shear reinforcement

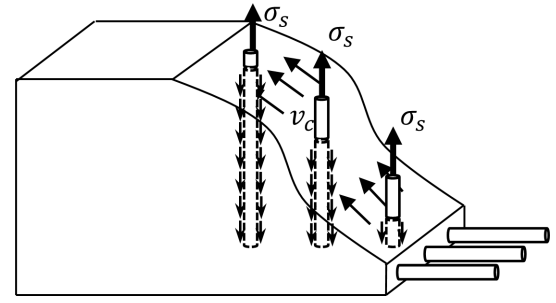


Fig. 4: Behaviour of bonded shear reinforcement at crack location

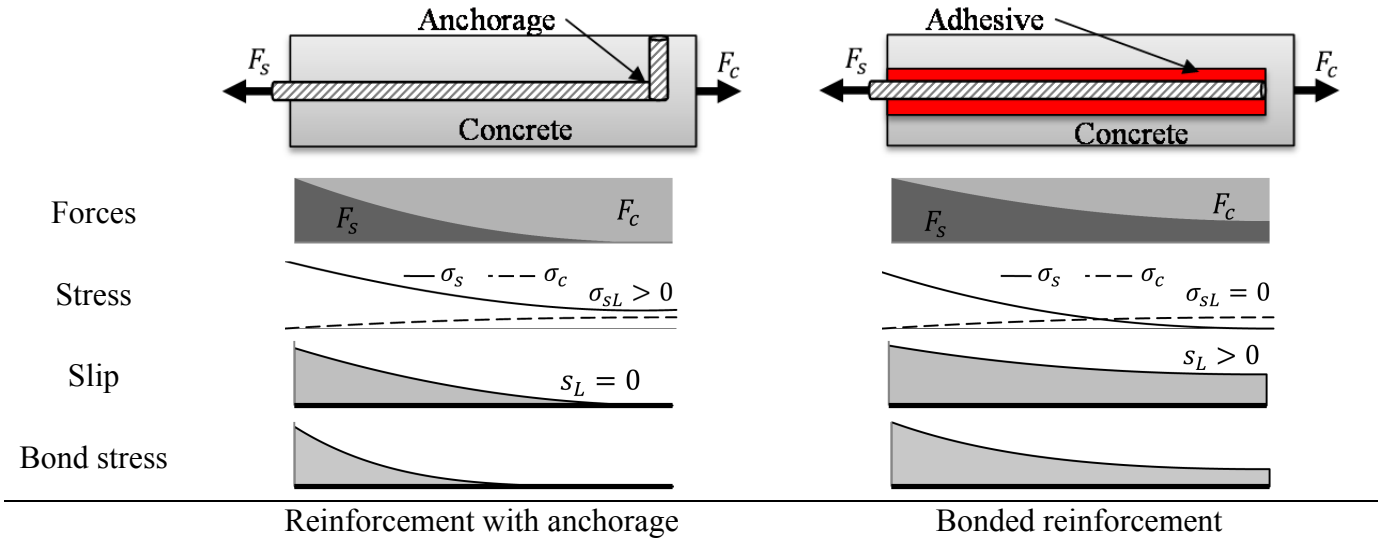


Fig. 5: Force, stress, slip and bond distribution along anchored and bonded reinforcing bars

BEHAVIOUR OF BONDED REINFORCING BARS

The behaviour of bonded reinforcing bars at a crack interface can be viewed as two pull-out tests, one on each side of the crack (Fig. 3 and 4). The maximum steel stress σ_s developed at the crack is function of the crack width, bond properties and the bar embedded length. Fig. 5 presents the difference in behaviour between bonded shear reinforcement and conventional stirrups. For stirrups, the extremities of the reinforcing bars are well anchored and hence can develop their yield resistances. At the extremities of the steel element, the displacement $s_L=0$ and the steel stress $\sigma_{sL}>0$. This is similar to the behaviour of a rebar between two cracks (Lee et al., 2010). For reinforcement bonded with the help of an adhesive, the axial stress has to be transferred from the steel to the surrounding concrete. Thus, at the rebar free extremity, $\sigma_{sL}=0$ and $s_L>0$. It can also be observed in Fig. 5 that the bond stress distribution is not constant along the rebar. The bond stress is function of the slip between the rebar and surrounding concrete which is function of the strains and the stresses developed in the two materials. Knowing the stress, strain and bond distribution, Equation 1 describes the relationship for the slippage “s” (Balázs, 1993; Lee et al., 2010).

$$\frac{d^2s}{dx^2} - \frac{4(1+n\rho)}{E_s d_b} \tau(s) = 0 \quad (1)$$

Where, n is the elastic modulus ratio of steel to concrete (E_s/E_c), ρ is the reinforcement ratio (A_s/A_c), and $\tau(s)$ is the local bond-slip behaviour at the interface.

Model for local bond stress relationship

The VecTor2 software is capable of predicting the response of concrete elements (Ghorbani-Renani et al., 2009; Vecchio 2004) and was chosen to model slabs strengthened with bonded reinforcing bars. This software uses two dimensional finite elements to model concrete structures, including a rotating smeared crack assumption, based on the Modified Compression Field Theory (MCFT) (Vecchio and Collins, 1986) and Disturbed Stress Field Model (DSFM) (Vecchio, 2000). Because current Canadian standards are based on MCFT, VecTor2 is a useful tool to undertake a study of the behaviour of strengthened slabs and to ultimately suggest a more adapted design method for future implement in Canadian standards. In addition, VecTor2 has the ability to define local bond-slip behaviour of the bar-concrete interface, according to pre-defined models (Eligehanson et al, 1983; Harajli et Mukaddam, 1988) or by defining an alternative model.

Comparison with experimental pull-out tests

Pull-out tests with embedded length between 13 mm and 500 mm were carried out to determine the bond stress – slip behaviour of the epoxy adhesive used as the bonding agent at the rebar-concrete interface. The concrete mix and steel reinforcing bars used were the same as those in the tested slab. Figure 6 presents the experimental bond-slip relationship of the epoxy adhesive. For comparison purposes, predefined VecTor2 local bond-slip models (Eligehanson, Harajli) and the *fib* model code 2010 bond slip model (*fib*, 2013) for the concrete-steel interface are also shown in Fig. 6.

The pull out test was performed on a 15M rebar with a 30mm embedded length. The concrete compressive strength of this test was 46 MPa. The resulting maximum bond strength was 30.85 MPa at a slip of 0.77 mm. The post-peak fracture energy determined between the slip at τ_{max} and the maximal displacement was 169 N-m. It can be seen that the pre-defined models for the concrete-steel interface do not adequately predict the bond behaviour of the concrete-epoxy-adhesive-steel interface. The bond-slip behaviour of the adhesive is stiffer than the pre-defined models. Moreover, the maximum bond stress of the epoxy adhesive is not well modelled. The experimental bond strength is about 30.85 MPa at 0.77 mm whereas the prediction using the Eligehausen model is about 19.80 MPa at 1.24 mm. Likewise, the post peak behaviour of both pre-defined models shows a higher slip and residual friction bond stress compared to experimental result. Thus, predefined bond-stress relationships in VecTor2 are not suitable to model the local behaviour of the tested adhesive for the concrete-epoxy-steel interface.

Proposed local bond-slip model

In order to increase the accuracy of the bond-slip behaviour considered in the FE model and future design calculations, a trilinear bond relationship is suggested (Fig. 7 and Equations 2 to 4). The first linear branch of the bond-slip relationship describes the ascending behaviour and the parameters were chosen to best represent the average pre-peak stiffness. The second linear segment describes the constant peak behaviour and the third linear segment is defined in order to respect the fracture energy of the test.

$$s \leq s_1 \quad \tau = \tau_1 \left(\frac{s}{s_1} \right) \quad (2)$$

$$s_1 < s \leq s_2 \quad \tau = (\tau_{max} - \tau_1) \left(\frac{s - s_1}{s_2 - s_1} \right) + \tau_1 \quad (3)$$

$$s > s_2 \quad \tau = \tau_{max} - (\tau_{max} - \tau_f) \frac{s - s_2}{s_3 - s_2} \geq \tau_f \quad (4)$$

Besides the trilinear model, another bond model which showed also a good fit with the experimental behaviour was introduced to solve the governing Equation 1. This suggested exponential model (Equa-

tions 5 and 6) is based on the work of Cosenza et al (1997). The parameter s_r and K must be calibrated according to experimental results. Figure 8 and Table 2 present in more detail the exponential and the trilinear bond-slip model for the epoxy adhesive that was used.

$$s \leq s_2 \quad \tau = \tau_{\max} \left(1 - e^{\left(\frac{-s}{s_r} \right)} \right) \quad (5)$$

$$s > s_2 \quad \tau = (\tau_{\max} - \tau_f) e^{\left(\frac{s_2 - s}{K} \right)} + \tau_f \quad (6)$$

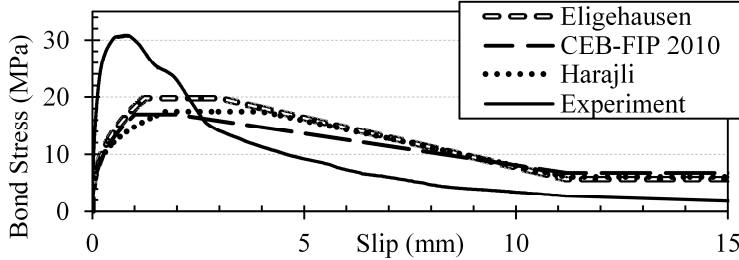


Fig. 6: Bond-slip behaviour of epoxy adhesive and comparison with predefined models

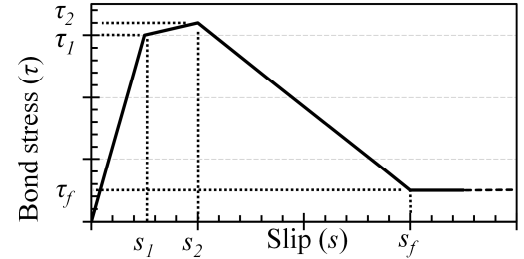


Fig. 7: Specific trilinear bond-slip relationship in VecTor2

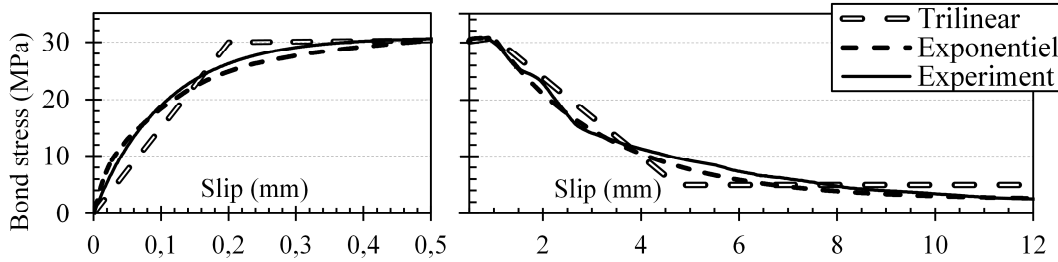


Fig. 8: Bond-slip suggested models and comparison with experimental pull-out test

Table 2: Parameters for trilinear and exponential bond-slip models

	τ_1 (MPa)	τ_{\max} (MPa)	τ_f (MPa)	s_1 (mm)	s_2 (mm)	s_3 (mm)	s_r (mm)	K (mm)
Trilinear	30	30.85	5	0.2	1	4.73	-	-
Exponential	-	30.85	2	-	1	4.73	0.105	2.373

DESCRIPTION OF FE MODEL FOR SLABS

A study of bonded shear strengthened slabs, including the trilinear bond-slip model, was performed with VecTor2. Slabs were modelled with 2D membrane elements. The longitudinal reinforcing bars and shear reinforcement were modelled with discrete truss elements. Conventional stirrups were modeled considering perfect bond between the truss elements and the surrounding concrete whereas contact elements were used between the steel and concrete elements for the epoxy bonded reinforcement.

Basic program options were selected for the material properties. The steel behaviour is modelled with a trilinear stress-strain relationship. The concrete compression behaviour is model according to the model suggested by Hoshikuma et al. (1997) and takes into account lateral confinement and compression softening. In tension, the behaviour is linear up to the tensile strength and the post-peak behaviour is represented with a linear law driven by the cracking energy G_f . The tension stiffening effect is also included according to the model of Lee & al. (2010). This model takes into account the tension stiffening after the yielding of the steel reinforcement. All relevant equations and complete references can be found in the VecTor2 reference manual (Wong and Vecchio, 2002).

RESULTS AND DISCUSSION

Experimental cracking patterns and FE prediction

Several analyses have been performed according to the various reinforcement layouts presented in Table 1. Figures 9 and 10 show the experimental cracking pattern of slabs B3 and B4 and the associated FE predictions. For comparison purposes, the results for slab S1 containing conventional stirrups are also presented. In a smeared crack model, each element (integration point) reaching the concrete tensile strength will exhibit a crack. However the ones with wider openings (main cracks) are illustrated in bold in Fig. 10. Figures 9 and 10 show good correlation between the FE model predictions and the experimental cracking patterns.

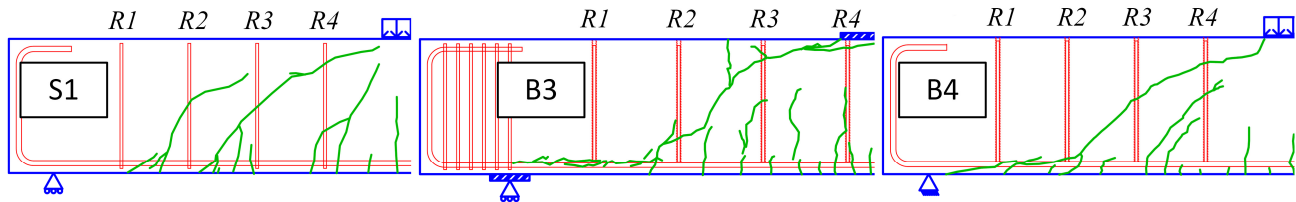


Fig. 9: Experimental cracking, slabs with stirrups (S1) and epoxy bonded reinforcement (B3-B4)

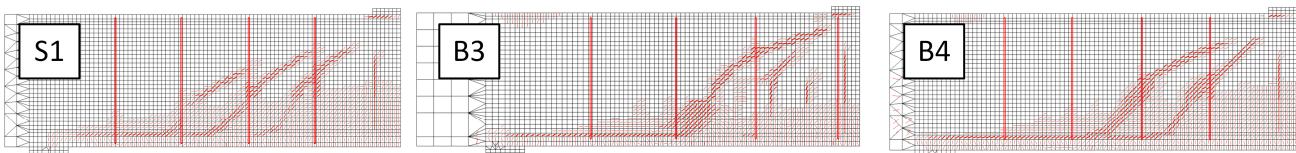


Fig. 10: FE cracking prediction, slabs with stirrups (S1) and epoxy bonded reinforcement (B3-B4)

Experimental shear carrying capacity and comparison to CSA code and FE model

Table 3 shows a summary of experimental and numerical results as well as predictions using the Canadian code approach. It can be seen that using the code equations and assuming that the epoxy bonded shear reinforcement acts as conventional stirrups results in unconservative predictions. However, by taking into account the bond behaviour, the predicted shear strengths by the FE model are close to the experimental results. VecTor2 predicts almost the same shear capacity for slab B3 as the experiment. Likewise, with an average experimental and a FE prediction shear capacity of 755.6 and 718.7 respectively, the FE model estimates the shear capacity of slab B4 within 5%. For all shear strengthened slabs with epoxy bonded reinforcement, the average of the predicted shear capacities divided by the experimental capacities was 1.016 and the coefficient of variation was 0.063. The shear strength provided by the shear reinforcement (V_s) is determined knowing the reinforcing bars area and the steel stress at the main shear crack. The concrete contribution to shear strength V_c is the difference between the total shear strength and the steel strength contribution. By comparing the standard V_{S-CSA} and the FE V_{S-FE} predictions, it can be observed that V_{S-CSA} is overestimated by the current standard for the strengthened slabs assuming fully bonded reinforcement. For slab B3 with shear reinforcement spacing of 470 mm, V_{S-FE} is below the fully bonded prediction by 25.4%. The concrete contribution V_{C-FE} predicted by FE model is also 51.2% below the concrete contribution estimated by the current standard V_{C-CSA} for this slab. With a closer spacing of shear reinforcement of 370 mm in slab B4, the strength predictions (standard versus FE) are closer. The standard overestimates the steel (V_{S-CSA}/V_{S-FE}) and concrete contribution (V_{C-CSA}/V_{C-FE}) of slab B4 by about 5.7% and 28.2% respectively. Indeed, with closer shear reinforcement spacing, the likelihood for a main shear crack to intercept a reinforcing bar in its central portion is increased. Thus, more bars are able to develop their yield strength and V_s is closer to the standard predictions assuming fully bonded reinforcement. In the case of stirrups, the reinforcement is well anchored and is able to develop its full yield strength which may not be the case for short embedded lengths of epoxy

bonded reinforcement. The embedment lengths for the slab B3 bars are presented in Table 4 and the bar stresses extracted from either the experiments or the FE results. Knowing the rebar numbering previously presented in Fig. 9, it can be observed that the axial steel stress predicted by VecTor2 for the shorter embedded length bonded reinforcing bar (bar R3) is below the steel yield strength of 480 MPa.

Table 3: Comparison between experimental, Canadian standard and VecTor2 results

Slabs	Test number	V_{exp} [kN]	V_{CSA} [kN]	V_{S-CSA} [kN]	V_{C-CSA} [kN]	V_{FE} [kN]	V_{S-FE} [kN]	V_{C-FE} [kN]
B3	1	490.3	700.8	350.2	350.6	506.8	289.9	216.9
	2	505.2	711.8	348.8	363.0	526.2	268.4	257.8
B4	1	742.3	828.0	441.1	386.9	718.7	417.0	301.7
	2	768.8	828.0	441.1	386.9	718.7	417.0	301.7

Table 4: Embedded length of epoxy bonded shear reinforcement of slab B3

Slab	Test number	Rebar number	Experimental		VecTor2		
			Embedded length (mm)	Max Steel Stress* (MPa)	Embedded length (mm)	Steel Stress (MPa)	Max Steel Stress* (MPa)
B3	1	R2	132	690	125	480.0	690
		R3	36	278	44.3	244.2	342
	2	R2	121	690	150	480.5	690
		R3	46	355	44.3	190.4	342

*Maximum steel stress according to the matlab model and the exponential bond behaviour, for the experimental embedded length.

EFFECT OF BOND AND SLIP ON SHEAR RESISTANCE

Model description

In order to study the effect of bond on shear resistance mechanisms and the distribution of stresses and slip along a bar, a reference tool was developed. This tool numerically solves the governing bond Equation 1 with the help of matlab. Unlike VecTor2, this matlab tool enables the slip, bond stress and steel stress distribution along a bonded rebar to be determined for different local bond-slip relationships. For this particular study, the exponential (Equations 5 and 6) local bond-slip relationship is used. Because the matlab model can make use of a much refined mesh (5000 linear elements instead of few elements in the VecTor2 mesh models), the prediction of stresses and slip along the bar is more precise. Moreover, the exponential bond-slip relationship used is better correlated to the experimental bond-slip relationship than the trilinear model used in VecTor2 (FE). Thus, the predicted behaviour is expected to be closer to the experimental behaviour. Therefore, this matlab bond model is used as a reference model for bond-slip behaviour along an epoxy bonded reinforcing bar.

Embedded length and maximum axial steel stress

Table 4 presents the embedded lengths and the maximum axial stress in the bar according to the matlab bond model. The determined maximum axial stress is limited by the bond along the rebar and the ultimate steel strength ($f_{uv}=690$ MPa). It can be observed that, for long embedded lengths, the maximal axial stress is limited by the steel strength f_{uv} . However, for the epoxy bonded shear reinforcement numbered R3, the embedded length is too short to develop the yield strength and the maximum steel axial stress is therefore limited by bond.

According to the VecTor2 model (FE), the slab B3 failure mode results from the yielding of shear reinforcement R2 while the axial stress in shear reinforcement R3 is lower than the maximum value of 342

MPa. This result can be explained by the crack width and the aggregate interlock mechanism. At steel yielding, the crack width increases rapidly and the shear strength provided by aggregate interlock (v_c) decreases (Equation 7). Thus, the maximum shear carrying capacity can be reached before the maximum steel stress can be developed in all the epoxy bonded shear reinforcement intercepting the main shear crack.

Axial steel stress at failure

Figure 11 presents the loading predictions by the matlab model of a bonded rebar (15M) according to two different embedded lengths of 40 and 130 mm. In a concrete element subjected to shear and associate diagonal crack, the slip of rebar is related to the crack width in the vertical direction. Referring to Fig. 3 and 9 where bars with various embedded lengths cross main diagonal cracks, figure 11 presents the axial stress-slip behaviour associated to two rebars with different embedded length. Figure 11 shows that, for the shorter embedded length, the maximum steel stress reached at 1 mm slip is under the ultimate strength of 690 MPa. For the longer embedded lengths, yield strength (480 MPa) and ultimate steel strength are reached at about 0.16 mm and 1.5 mm, respectively. The combined maximum shear capacity provided by the bonded shear reinforcement is reached at an intermediate slip of 1.05 mm. Also, Fig. 11 shows that, when yielding of the 130 mm embedded length bar is reached, the steel stress in the other rebar is 231 MPa. It may be underlined that this value is similar to the steel stresses determined by Vector2 for bar “R3” in slab 3 (shorter embedded lengths of 36 and 46 mm) of 244.2 MPa and 190.4 MPa.

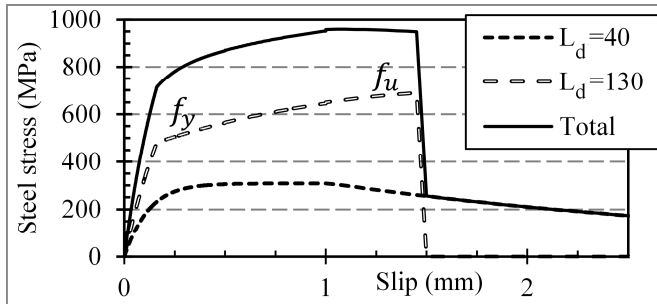


Fig. 11: Steel stress function of applied slip for short and long embedded length

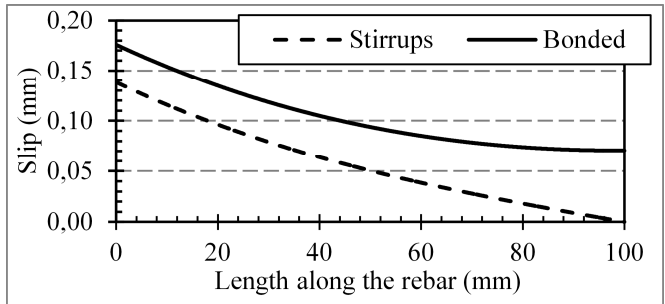


Fig. 12: Slip along full anchored bar or bonded bar, applied stress 480 MPa

$$v_c = \frac{\sqrt{f_c}}{0.31 + \frac{24w}{a_g + 16}} \quad (7)$$

$$w = s_\theta \varepsilon_1 \quad (8)$$

Effect of anchorage on aggregate interlock

Fig. 12 shows the slip distribution along a fully anchored bar (stirrup) and an epoxy bonded bar. The model assumes no displacement and no steel stress at the rebar extremity as stated previously in Fig. 5. The results showed in Fig. 12 concern a 15M rebar pull out test with an equivalent loading of 480 MPa (corresponding to yielding) with an embedded length of 100 mm. As expected, for the same applied stress, the slip of the bonded bar is larger than the fully anchored one. Since for shear cracks, the crack width partly depends on the shear reinforcement slip, it is also expected that the crack width of epoxy bonded shear strengthened slabs will be larger than cracks developed in slabs with fully anchored bars (stirrups).

The crack width can also be expressed as the product of crack spacing and the strain (Equation 8). Thus, for the same bar tensile strain, the crack spacing should be larger for bonded reinforcement. This is ob-

served through the cracking pattern of Fig. 9 and 10. Slab S1 reinforced with stirrups have experienced more shear cracks than slabs B3 or B4 strengthened with epoxy bonded shear reinforcement. By knowing that the aggregate interlock capability decreases with wider cracks, the concrete contribution V_C should be affected in a similar way. That may explain why the concrete contributions presented in Table 3 are lower than the CAN-CSA standard predictions assuming fully bonded reinforcement. Thus, it is also expected that the provisions of current standards will result in an overestimation of V_C when epoxy bonded shear reinforcement is used as a strengthening technique.

CONCLUSION AND FUTURE WORK

The main goal of this research is to develop models capable of predicting the increase in shear strength of thick slabs strengthened with epoxy bonded shear reinforcement. Post-installed shear reinforcing bars were inserted in drilled-in holes and bonded to the concrete with an epoxy adhesive. This paper presents the influence of the anchorage conditions on the efficiency of this shear strengthening technique. For conventional stirrups, well anchored conditions exist and, at locations where a crack intercepts the stirrups, the stirrups are able to develop their full yield strength. For epoxy bonded shear reinforcement, the diagonal main shear crack defines the embedment length of the rebars. Therefore, the stress carried by these rebars can be limited by the bond strength.

Pull-out tests have been carried out to determine the local bond-slip relationship of concrete-epoxy adhesive-steel interface. This behaviour has been introduced in the FE software VecTor2 to model shear strengthened slabs with epoxy bonded reinforcement. It appeared that VecTor2 pre-defined bond-slip models for the concrete-steel interface were not able to reproduce the epoxy adhesive behaviour. Thus, two proposed models were judged adequate to reproduce the adhesive behaviour. A simple trilinear relationship was used for the FE models of slabs and a more precise exponential relationship was used to compare the slip, bond stress and axial steel stress distributions along the bonded rebars. After the FE analysis of slabs with epoxy bonded rebars and analysis of the bond-slip properties, the following conclusions can be drawn:

- With an adequate bond model, a good correlation between numerical and experimental results can be obtained;
- The current CAN-CSA standard, assuming fully bonded reinforcement, overestimates both the steel contribution V_S and the concrete contribution V_C components of the shear capacity;
- With smaller shear reinforcement spacing, the main shear crack intercepts more bars in their mid-height region enabling them to develop their yield strength. Therefore the V_S contribution to shear capacity is closer to standard predictions assuming fully bonded reinforcement;
- The maximum axial rebar capacity is driven by bond properties for short embedded length and limited by the steel strength for long embedded lengths and hence the maximum capacity of each epoxy bonded reinforcing bar is not necessarily reached at slab failure;
- The slip of shear reinforcement at a crack location is larger for epoxy bonded bars than for well anchored stirrups. Thus for such larger crack widths, the aggregate interlock capability is reduced.

Even if the experimental program has demonstrated the efficiency of post-installed shear reinforcement bonded to the concrete structure, the “stirrups design procedure” in the current standard should not be used for drilled-in bonded shear reinforcement. The next step of this research program will be to develop

a design method for the this shear strengthening technique taking into account the effect of bond-slip behaviour on the V_S and V_C shear capacity components.

ACKNOWLEDGMENT

The Research reported in this paper was made possible by the funding from the Natural Sciences and Engineering Research Council of Canada (NSERC) and the “Fonds de Recherche du Québec – Nature et Technologies” (FRQNT). The authors wish also to acknowledge the work of Philippe Provencher, Benoit Cusson and Felix-Antoine Villemure who performed the experimental slabs tests and the pull-out tests during their master project.

SYMBOLS

a_g	Aggregate size	E_c	Elastic modulus of concrete (initial tangent stiffness)
b	Slab width	E_s	Elastic modulus of steel
d	Effective flexural depth	F_c	Force in concrete
d_b	Reinforcing bar diameter	F_s	Force in steel
d_v	Effective shear depth, taken as the greater of $0.9d$ and $0.72h$	G_f	Cracking energy
f_c	Cylinder concrete compressive strength	L_b	Embedded length
f_{yv}	Yield strength of shear reinforcement	V_c	Shear carrying capacity provides by concrete
h	Slab height	V_s	Shear carrying capacity provides by shear reinforcement
n	Ratio of elastic modulus (E_s/E_c)	ε_1	Principal tensile strain
s	Slip, relative displacement between concrete and steel interface	ρ	Reinforcement ratio (A_s/A_c)
s_v	Spacing of shear reinforcement	ρ_{flex}	Reinforcement ratio of flexural reinforcement ($A_s/(d b)$)
s_θ	Crack spacing inclined at principal tensile stress angle	σ_c	Axial stress in concrete
v_c	Shear stress in concrete	σ_s	Axial stress in steel
w	Crack width	τ	Bond stress
A_v	Area of all shear reinforcement within a distance s_v	τ_f	Residual bond strength (friction)
		τ_{max}	Maximum bond strength

REFERENCES

- Adhikary, B.B. and Mutsuyoshi, H. (2006), “Shear strengthening of reinforced concrete beams using various techniques”, *Construction and Building Materials*, Elsevier, No. 20, 366-373.
- Balázs, G. L. (1993), “Cracking Analyse Based on Slip and Bond Stress”, *ACI Materials Journal*, Vol. 90, No. 4, 340-348.
- Barros, J.A.O. and Dias, S.J.E. (2006), “Near surface mounted CFRP laminates for shear strengthening of concrete beams”, *Cement & Concrete Composites*, Elsevier, No. 28, 276-292.
- CAN-CSA, Canadian Standards Association (2006), “Canadian Highway Bridge Design Code” CAN-CSA S6-06, 768 p.
- Cosenza, E., Manfredi, G., and Realfonzo, R. (1997). “Behavior and modeling of bond of FRP rebars to concrete.” *J. Compos. for Constr.*, ASCE, Vol. 1 No. 2, 40–51.
- Cusson, B. (2012), “Renforcement des dalles épaisses en cisaillement”, (Master Thesis – in French) Civil Engineering department, Université Laval, Québec, Canada, 119p.

- De Lorenzis, L. and Nanni, A. (2001), "Shear Strengthening of Reinforced Concrete Beams with Near-Surface Mounted Fiber-Reinforced Polymer Rods", *ACI Structural Journal*, Vol. 98, No. 1, pp. 60-68
- Eligehausen, R., Popov, E. and Bertero, V. (1983), "Local Bond Stress-Slip relationship of Deformed Bars under Generalized Excitations", Report No. UCB/EERC-83/23, Earthquake Engineering Center, University of California, Berkeley.
- Fernández-Ruiz, M., Muttoni, A. and Kunz, J. (2010), "Strengthening of Flat Slabs Against Punching Shear Using Post-Installed Shear Reinforcement", *ACI Structural Journal*, Vol. 107, No. 4, 434-442.
- fib* – International Federation for Structural Concrete (2013), "Model Code for Concrete Structures 2010". 402p.
- Fiset, M., Bastien, J. and Mitchell, D. (2012), "Post-Installed Shear Reinforcement for Concrete Thick Slabs", *The 9th fib International Ph.D. Symposium in Civil Engineering*, Karlsruhe, Germany 115-121
- Ghorbani-Renani, I., Veley, N., Tremblay, R., Palermo, D., Massicotte, B. and Léger, P. (2009), Modeling and testing Influence of Scaling Effects on Inelastic Response of Shear Walls", *ACI Structural Journal*, Vol. 106, No. 3, 358-367
- Harajli, M.H. and Mukaddam, M.A. (1988), "Slip of Steel Bars in Concrete Joints under Cyclic Loading", *Journal of Structural Engineering*, ASCE, Vol. 114, No. 9, 2017-2035.
- Hoshikuma, J., Kawashima, K., Nagaya, K. and Taylor, A.W. (1997), "Stress-Strain Model for Confined Reinforced Concrete in Bridge Piers", *Journal of Structural Engineering*, ASCE, Vol. 123, No. 5, 624-633.
- Johnson, P. M., Couture, A., and Nicolet, R. (2007), "Commission of inquiry into the collapse of a portion of the de la Concorde overpass", Library and National Archives of Quebec. 222p.
- Lee, S.C., Cho, J.Y. and Vecchio, F.J. (2011), "Model for post-yield tension stiffening and rebar rupture in concrete members", *Engineering Structures*, Elsevier, Vol. 33, 1723-1733.
- Mitchell, D., Marchand, J., Croteau, P. and Cook, W. D. (2011), "Concorde Overpass Collapse: Structural Aspects", *Journal of Performance of Constructed Facilities*, ASCE, Vol. 25, No. 6, 545-553.
- Provencher, P. (2011), "Renforcement des dalles épaisses en cisaillement", (Master Thesis – in French) Civil Engineering department, Université Laval, Québec, Canada, 142p.
- Vecchio, F.J. (2000), "Disturbed Stress Field Model for Reinforced Concrete: Formulation", *Journal of Structural Engineering*, ASCE, Vol. 126, No.9, 1070-1077.
- Vecchio, F.J. (2004), "Experimental and Analytical Reexamination of Classic Concrete Beam Tests", *Journal of Structural Engineering*, ASCE, Vol. 130, No. 3, 460-469.
- Vecchio, F.J. and Collins, M.P. (1986), "The Modified Compression Field Theory for Reinforced Concrete Elements Subjected to Shear", *ACI Journal*, Vol. 83, No.2, 219-231.
- Wong, P. S. and Vecchio, F. J.(2002)"VecTor2 and FormWorks User's Manual", {www.civ.utoronto.ca/vector}, 213p